Am J Transl Res 2021;13(3):1483-1493
www.ajtr.org /ISSN:1943-8141/AJTR0115809

Original Article

Astaxanthin provides neuroprotection in an experimental model of traumatic brain injury via the Nrf2/HO-1 pathway

Fei Gao[1*], Xiao Wu[2*], Xiang Mao[3,4,5,6,7*], Fei Niu[4,5,6,7], Bin Zhang[1], Jinqian Dong[1], Baiyun Liu[1,5,6,7]

[1]Beijing Tiantan Hospital, Capital Medical University, Beijing, 100070, China; Departments of [2]Emergency, [3]Neurosurgery, The First Affiliated Hospital of Anhui Medical University, Hefei 230022, Anhui, China; [4]Beijing Neurosurgical Institute, Capital Medical University, Beijing 100070, China; [5]Beijing Key Laboratory of Central Nervous System Injury, Beijing Neurosurgical Institute, Capital Medical University, Beijing 100070, China; [6]Nerve Injury and Repair Center of The Beijing Institute for Brain Disorders, Beijing 100070, China; [7]China National Clinical Research Center for Neurological Diseases, Beijing 100070, China. [*]Equal contributors and co-first authors.

Received June 7, 2020; Accepted December 18, 2020; Epub March 15, 2021; Published March 30, 2021

Abstract: Background: Astaxanthin (ATX) is a carotenoid pigment with effective antioxidant, anti-inflammatory, antitumor and immunomodulatory actions. ATX has been proposed to exert neuroprotective effects and attenuate oxidative stress in mice after traumatic brain injury (TBI). The nuclear factor erythroid 2-related factor 2 (Nrf2)-heme oxygenase 1 (HO-1) signaling pathway is stimulated after TBI and activates a compensatory mechanism against TBI. Nevertheless, the effect of ATX on the pathophysiology of TBI in mice is limited. Our present study evaluated the neuroprotection afforded by ATX and the possible role of the Nrf2/HO-1 pathway in experimental TBI. Materials and methods: Mice were casually separated into 3 groups: the sham, TBI + vehicle, and TBI + ATX (100 mg/kg, intraperitoneally administered) groups. Neurobehaviors of the mice were assessed using the neurological severity scores (NSSs), the forced swimming test (FST) and the rotarod test. Levels of the Nrf2, HO-1, NAD(P)H: quinine oxidoreductase-1 (NQO1), cleaved caspase3 (C-caspase3), and superoxide dismutase1 (SOD1) proteins and levels of the Nrf2 and HO-1 mRNAs were assessed. In addition, Nrf2 nuclear import and apoptosis were measured after TBI. Results: The ATX treatment significantly improved the neurological status, promoted Nrf2 activation, and upregulated the expression of the Nrf2 and HO-1 mRNAs and the levels of the Nrf2, HO-1, and NQO1 proteins after TBI. The level of the SOD1 protein was decreased after TBI and increased after ATX treatment; however, the difference was not significant. ATX markedly reduced the level of the C-caspase3 protein and the number of TUNEL-positive cells, indicating that it exerted an antiapoptotic effect. Immunofluorescence staining confirmed that ATX promoted Nrf2 nuclear import. Conclusions: Based on our study, ATX possibly affords neuroprotection by activating the Nrf2/HO-1 signaling pathway in mice after TBI.

Keywords: Astaxanthin, traumatic brain injury, neuroprotection, Nrf2/HO-1 pathway

Introduction

Traumatic brain injury (TBI) is currently main cause of neurological dysfunction and death in developed and developing countries. It causes long-term and short-term complications, leads to large economic losses worldwide and imposes a substantial social burden [1, 2]. The mechanisms underlying neural injury caused by TBI mainly include the complex pathological mechanisms of primary injury and secondary injury [3, 4]. Primary injury is generally caused by accidents such as explosions, car accidents, falls from heights, and other falls, and few interventions are available for primary injury. Secondary injury is a more complicated and long-term process that is based on the primary injury [5]. Its main pathological mechanisms include oxidative stress, the response to inflammation, and cell death, which eventually lead to neuronal dysfunction and death [6-8]. Based on accumulating evidence, oxidative stress and inflammatory responses are the keys to secondary injury after TBI [9-12]. Therefore, many researchers have explored the underlying mechanisms of oxidative stress and

the response to inflammation after TBI to identify targets for neuroprotection.

Nuclear factor erythroid 2-related factor 2 (Nrf2) is a transcription factor that plays an important role in upregulating the expression of antioxidant genes in response to oxidative stress [13]. In the absence of stress, Nrf2 is bound to Kelch-like ECH-associated protein 1 (Keap1) in the cytoplasm and is transported to the ubiquitin-proteasome system for degradation [14, 15]. Upon exposure to stress, Nfr2 is transported to the nucleus, heterodimerizes with small Maf proteins, and activates the transcription of antioxidant genes such as heme oxygenase 1 (HO-1) and quinine oxidoreductase 1 (NQO1) to increase the cellular antioxidant and anti-inflammatory capabilities [16-18]. The Nrf2 signaling pathway exerts neuroprotective effects by playing a key role in antioxidant and anti-inflammatory responses after TBI [19-21]. Moreover, the loss of Nrf2 aggravates oxidative stress after TBI in mice [22]. Therefore, the Nrf2 signaling pathway is a new therapeutic target for TBI.

Astaxanthin (ATX), which is naturally present in many organisms, particularly organisms living in the marine environment, is a red carotenoid pigment common found in many types of seafood (such as salmon, shrimp, lobster and crayfish) that functions as a powerful biological antioxidant [23]. The use of ATX in food coloring, natural feed additives to natural feed applied in the poultry industry and aquaculture, particularly as a feed supplement for salmon, trout and shrimp farming, is increasing. ATX exhibits high bioavailability and safety, and little data on the toxicity or harmful effects of ATX have been reported. A clinical study showed that high-dose ATX (40 mg daily) does not exert any harmful effects when administered for 4 weeks as a treatment for *Helicobacter pylori* [24]. ATX is converted into a more stable product in the body and terminates free radical chain reactions to function as a strong antioxidant [25]. ATX has the potential to promote health by preventing and treating various diseases, such as oxidative stress-related disorders, inflammatory diseases, cancer, and diabetes, and by protecting the cardiovascular system, gastrointestinal system, liver, nerves, eyes and skin [26]. Therefore, ATX has considerable prospective applications in the areas of human health and nutrition and is considered to have great potential to protect organisms from various diseases [25, 27, 28].

ATX, a red carotenoid, has various biological functions, such as antioxidant, anti-inflammatory, antitumor, and immunomodulatory activities [29, 30]. ATX has been shown to alleviate brain damage in a rat model of subarachnoid hemorrhage through the Nrf2 signaling pathway [31]. In addition, other studies have found that ATX improves cognition and alleviates brain edema in mouse models of TBI [32, 33]. However, the neuroprotective mechanism of ATX in TBI is unclear. In this study, we assessed the neuroprotective properties of ATX and the possible role of the Nrf2/HO-1 pathway in a mouse model of TBI.

Materials and methods

Animals

We purchased male C57BL/6N mice (18-22 g) from Charles River Company (Beijing, China). The animals were provided free access to water and food for 2-3 days before testing.

Models of TBI

A mouse model of moderate controlled cortical impact (CCI) TBI was constructed with a cortical impactor (PCI3000, USA) as described previously [34, 35]. First, isoflurane was used to anesthetize the mice that were fixed on a stereotactic instrument. Isoflurane was continuously administered to maintain the anesthetic plane, 75% alcohol was used to disinfect the skin on the head of each mouse, the hair on the head was shaved, and a 1-cm incision was made along the midline of the scalp. Finally, the skin and periosteum were retracted from the skull surface; a 4-mm^2 craniotomy was performed on the right parietal bone, with the medial edge located 2 mm lateral to the midline, without disrupting the dura. A single impact was delivered by contacting the surface of the mouse brain with a 2.5-mm impact head (bearing speed: 3.0 m/s, injury penetration: 1.0 mm, dwell time: 150 ms), resulting in moderate brain injury. The mouse skull was returned and glued, the skin on the head was sutured, and anesthesia was terminated after the impact. After the mice awoke, they were returned to the breeding room and provided free access to

water and food. The same procedure, including anesthesia and craniotomy, but without the impact was performed on the sham-operated mice.

Drugs and experimental groups

The assignment of mice into groups and the usage, dosage and administration of the drug (ATX) were performed in accordance with a previously published report. Mice used as controls were injected intraperitoneally with an equal amount of corn oil 30 minutes after CCI.

Behavioral evaluation

Neurological severity scores (NSSs): The NSSs of the mice from the sham, TBI + vehicle and TBI + ATX groups were assessed on post-trauma days (PTDs) 1, 3, and 7 (days 1, 3, and 7 after TBI) to evaluate behavioral changes. NSSs were assigned based on a scale ranging from 0-10 points (0 = minimum deficit and 10 = maximum deficit) [36] to evaluate the motor, sensory, reflex, and balance functions of mice. Higher scores indicated a more severe injury. The behavioral tests were conducted by two independent researchers who were blinded to the experimental groups.

Rotarod test: The rotarod test was used to assess the sensorimotor coordination and motor learning in the rodent models of central nervous system diseases. The test involves the coordination of the forelimbs and hindlimbs. Each mouse was placed on a rod rotating at a constant speed, and the latency to fall was recorded. During the preinjury training phase, the mice were subjected to five consecutive training trials in which the rod rotated at 10 rpm (rpm) for 5 minutes. After 24 hours, the mice were exposed to TBI and then tested on PTDs 1, 3, and 7. Each mouse was placed on the rod three times on each testing day, and the average latency to fall was recorded. If the mouse did not fall off the rod within a time span of 5 minutes, it was manually removed, and its latency to fall was recorded as 5 minutes.

Forced swim test (FST): The FST assesses the tendency of mice to surrender their efforts to escape from a hostile environment; fewer efforts to escape are viewed as indicating behavioral despair. The mice were subjected to the FST on PTD 7. The instrument was a transparent plastic bucket (15.7 cm in diameter and 23-cm high) filled with water (24-26°C) to a depth of 18 cm. The time each mouse spent floating in the water within a 6-minute period (immobility time, in seconds) and the latency (seconds) to when the mouse first exhibited immobility were recorded. The mice were considered immobile when they stopped struggling and floated in the water, making only the necessary movements to keep their heads above the water. Swimming was defined as strenuous exercise during which the front paws disrupted the surface of the water.

Brain tissue processing

On PTD 1, animals from the different groups were deeply anesthetized with chloral hydrate (4%, 10 ml/kg) and intracardially perfused with cold heparinized saline to collect tissues used for real-time quantitative PCR (RT-qPCR) and Western Blot. The area of the ipsilateral cortex located 3 mm from the edge of the contusion was collected and frozen immediately in liquid nitrogen; the specimen was then transferred to a -80°C freezer until use. The same tissue processing protocol was used for immunofluorescence and TUNEL staining, except that whole-brain tissues were placed in cold 4% paraformaldehyde immediately after perfusion with cold heparinized saline and stored in a 4°C refrigerator until use.

RT-qPCR

After TBI, total RNA was extracted from brain tissues collected 24 hours using TRIzol reagent (15596026, Invitrogen, USA). Reverse transcription was performed using the Prime-Script RT Reagent Kit (K1622, Thermo, USA). The following primers were used to amplify the target genes: Nrf2: F, 5'-TGAAGCTCAGCTCGCATTGA-3', R, 5'-TGCTCCAGCTCGACAATGTT-3'; HO-1: F, 5'-AAGCTTTTGGGGTCCCTAGC-3', R, 5'-GGCTGGATGTGCTTTTGGTG-3'; and GAPDH: F, 5'-TATGTCGTGGAGTCTACTGGT-3', R, 5'-GAGTTGTCATATTTCTCGTGG-3'. Primers were synthesized by General Biotechnology (Shanghai, China). The Quant Studio™ 5 System and SYBR™ Select Master Mix (4472908, Life Technologies, USA) were used for amplification, and expression levels were standardized to GAPDH.

Western blot

Proteins were extracted from brain tissues collected 24 hours after TBI using complete RIPA buffer (G2002, Servicebio, Wuhan, China) containing protease inhibitors (ab201115, Abcam,

USA) and an electric tissue homogenizer, followed by centrifugation for 30 minutes at 14,000 *g* at 4°C. After collecting the supernatants, a BCA kit (G2026, Servicebio, Wuhan, China) was used to determine protein concentrations. Thirty micrograms of protein from each sample were diluted with distilled water and 5x loading buffer, and the mixtures were heated in a bath at 100°C for 10 minutes. Then, the 30-μg protein samples were loaded onto a 10% or 12% polyacrylamide gel, electrophoretically separated, and electro-transferred onto polyvinylidene fluoride (PVDF) membranes. The membranes were blocked with 5% milk/Tris-buffered saline/0.05% Tween 20 (TBST) for 2 hours and then incubated at 4°C overnight with rabbit anti-Nrf2 (1:1,000, ab137550, Abcam, USA), rabbit anti-HO-1 (1:1,000, ab68477, Abcam, USA), rabbit anti-NQO1 (1:1,000, ab80588, Abcam, USA), rabbit anti-cleaved caspase3 (C-caspase3) (1:1,000, 9661, Cell Signaling Technology, USA), rabbit anti-superoxide dismutase 1 (SOD1) (1:1,000, 10269-1-AP, Proteintech Group, Inc., Wuhan, China,) and mouse anti-actin (1:1,000, GB12001, Servicebio, Wuhan, China) primary antibodies. The membranes were incubated with the appropriate secondary antibody for 1.5 hours at room temperature and then reacted with a hypersensitive luminescent liquid (G2014, Servicebio, Wuhan, China) after washes with TBST. Chemiluminescence was performed in a dark room, and the densitometry analysis was performed using ImageJ software.

Immunofluorescence staining

For immunofluorescence staining, three randomly selected fields were analyzed from stained 4-μm-thick coronal sections from each mouse at a magnification of 400×. First, paraffin sections were dewaxed and rehydrated, and antigen repair was performed with an EDTA (pH 8.0) antigen repair solution. Then, the sections were treated with an autofluorescence quenching agent, blocked with serum and incubated with a rabbit monoclonal anti-Nrf2 antibody (1: 200, ab137550, Abcam, USA) at 4°C overnight. On the next day, the sections were incubated with a fluorescent dye-conjugated secondary antibody (CY3-labeled goat anti-rabbit, 1:300, GB21303, Servicebio, Wuhan, China) for 1 hour at room temperature and counterstained with DAPI (G1012, Servicebio, Wuhan). The sections were washed with PBS between each incubation. A NIKON DS-U3 upright microscope (NIKON, Japan) was used to capture images that were subsequently evaluated with Image-Pro Plus 6.0 software (Media Cybernetics, USA) as previously reported.

TUNEL staining

After brain specimens were routinely embedded in paraffin, they were sliced into 4-μm-thick sections. Apoptotic cells were analyzed using the TUNEL Detection Kit (11684817910, Roche, USA). Using standard procedures, paraffin sections were first deparaffinized in water and then incubated with proteinase K working solution for repair. Afterwards, the sections were incubated with a permeabilization solution to permeabilize the membrane followed by a mixture of reagent 1 (TdT) and reagent 2 (dUTP) from the TUNEL staining kit. Finally, DAPI was used to counterstain the nuclei, and the sections were mounted with antifluorescence quenching agent. The sections were observed and images were captured using a fluorescence microscope (Nikon Eclipse C1). DAPI-stained nuclei appeared blue upon excitation with ultraviolet light, and TUNEL-stained cells were labeled with FITC and appeared green. Two researchers who were blinded to the groups analyzed the cells and calculated the mean percentage of TUNEL-positive cells in high-power fields. The number of cells in three random high-power fields from each section were calculated.

Statistical analysis

Data are displayed as the means ± SD and were evaluated using GraphPad Prism software (version 7.00, GraphPad Software, San Diego, CA, USA). Because of the size of the groups, nonparametrical tests were used for further analysis. The Mann-Whitney rank sum test was used for comparisons between two groups, and the Kruskal-Wallis test with Student-Newman-Keuls post hoc test was used for multigroup comparisons. Differences between groups were considered statistically significant at $P<0.05$.

Results

ATX improves the neural function of mice after TBI

All mice exhibited neurological dysfunction after TBI (**Figure 1A-D**). As shown in **Figure 1A**, the TBI + vehicle group showed a higher NSS

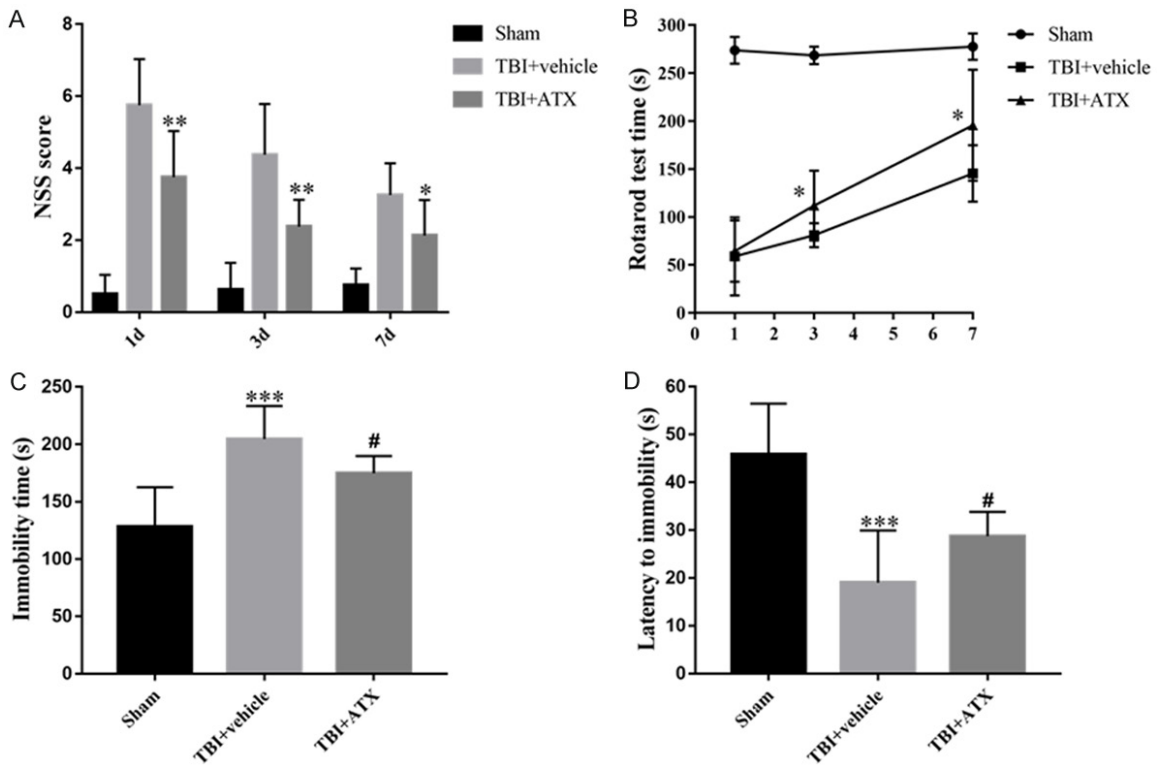

Figure 1. Astaxanthin improves neural function in mice after TBI. The NSS score (A) of the TBI + ATX group was lower than the TBI + vehicle group at PTDs 1 (P<0.01), 3 (P<0.01) and 7 (P<0.05) after TBI. In the rotarod test (B), significant improvements were detected in the TBI + ATX group at PTDs 3 (P<0.05) and 7 (P<0.05) after TBI. In the forced swim test (C, D), the time spent immobile within 6 minutes (C) was longer in the TBI + vehicle group than in the sham group at PTD 7 (P<0.001), and the TBI + ATX group recorded a reduced immobility time within 6 minutes compared with the TBI + vehicle group on PTD 7 (P<0.05). The latency to immobility (D) in the TBI + vehicle group was shorter than in the sham group on PTD 7 (P<0.001); however, the latency to immobility in the TBI + ATX group was longer than in the TBI + vehicle group on PTD 7 (P<0.05); n = 8 animals per group. *P<0.05, **P<0.01, and ***P<0.001 compared with the TBI + vehicle or sham group; $^{\#}P$<0.05 compared with the TBI + vehicle group.

score than the sham group; however, the TBI + ATX group showed a lower NSS score than the TBI + vehicle group on PTDs 1 (P<0.01), 3 (P<0.01) and 7 (P<0.05). The score of the sham group was approximately zero and did not change throughout the study. Similarly, as shown in **Figure 1B**, significant improvements in performance on the rotarod test were detected in the TBI + ATX group compared to the TBI + vehicle group on PTDs 3 (P<0.05) and 7 (P<0.05). As shown in **Figure 1C** and **1D**, the TBI + vehicle group exhibited a longer period of immobility within a 6-minute period in the FST than the sham group on PTD 7 (P<0.001). However, the TBI + ATX group exhibited a shorter immobility time within a 6-minute period than the TBI + vehicle group on PTD 7 (P<0.05). A shorter latency to immobility was observed for the TBI + vehicle group than the sham group on PTD 7 (P<0.001), whereas the latency to immobility of the TBI + ATX group was longer than the TBI + vehicle group on PTD 7 (P<0.05).

ATX promotes the nuclear import of Nrf2 one day after TBI

The results of immunofluorescence staining confirmed that Nrf2 was transported to the nucleus. In the sham group, Nrf2 immunoreactivity was very low, and Nrf2 was mainly located in the cytoplasm (**Figure 2A**). However, in the TBI + vehicle group, Nrf2 was partially transported to the nucleus, and Nrf2 immunoreactivity was stronger than in the sham group (**Figure 2B**, P<0.001). Nrf2 immunoreactivity was stronger in the TBI + ATX group than in the TBI + vehicle group on PTD 1 (**Figure 2B**, P<0.05).

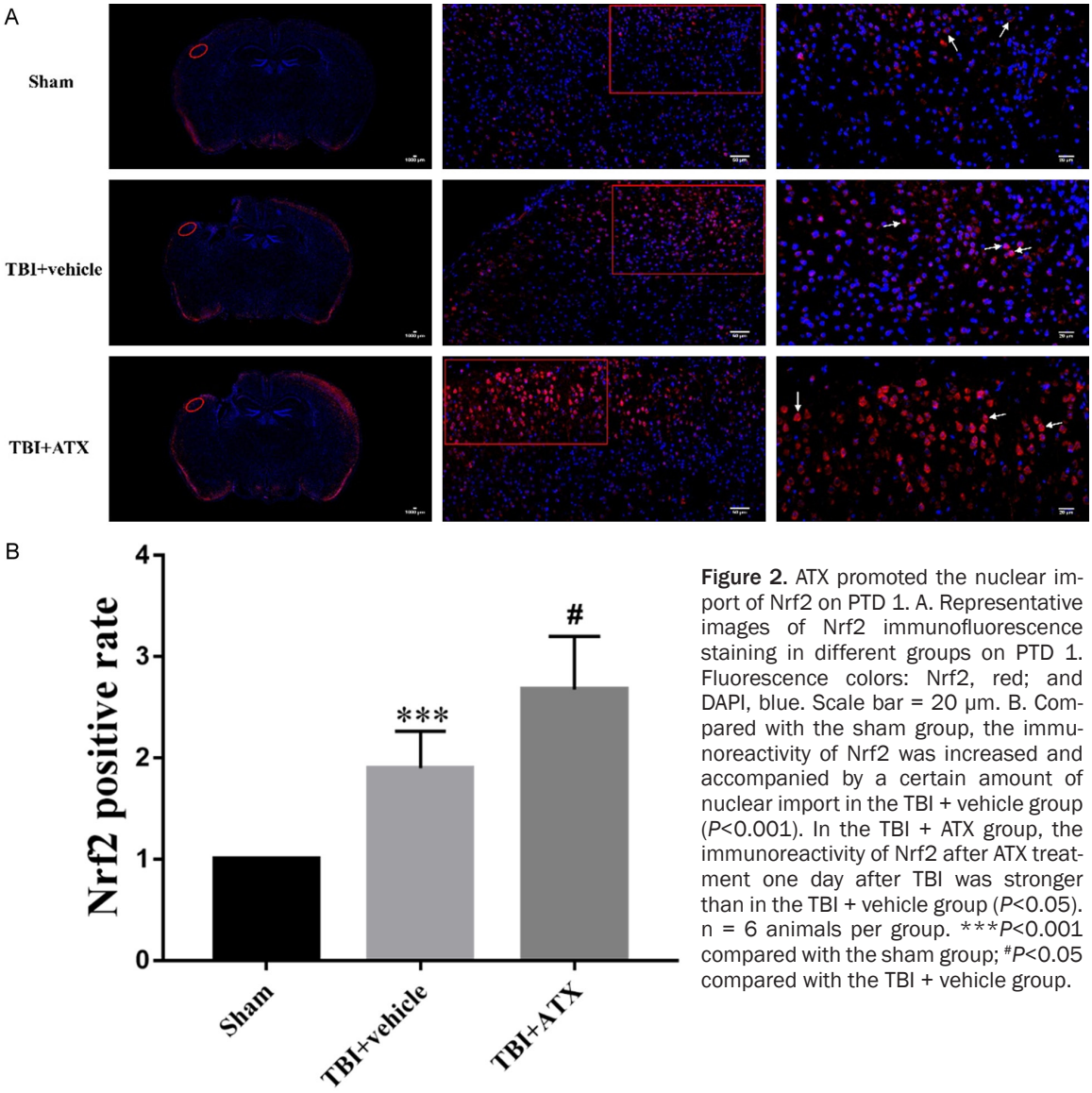

Figure 2. ATX promoted the nuclear import of Nrf2 on PTD 1. A. Representative images of Nrf2 immunofluorescence staining in different groups on PTD 1. Fluorescence colors: Nrf2, red; and DAPI, blue. Scale bar = 20 μm. B. Compared with the sham group, the immunoreactivity of Nrf2 was increased and accompanied by a certain amount of nuclear import in the TBI + vehicle group (P<0.001). In the TBI + ATX group, the immunoreactivity of Nrf2 after ATX treatment one day after TBI was stronger than in the TBI + vehicle group (P<0.05). n = 6 animals per group. ***P<0.001 compared with the sham group; $^{\#}P$<0.05 compared with the TBI + vehicle group.

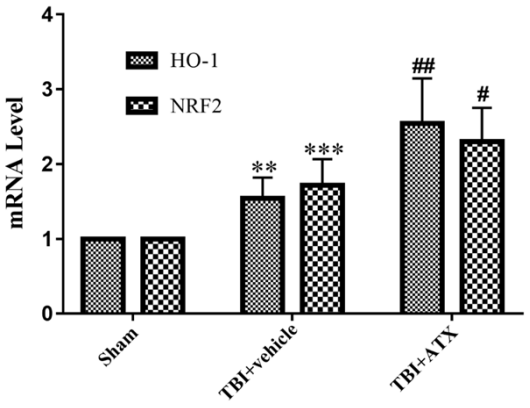

Figure 3. ATX increased the expression of the Nrf2 and HO-1 mRNAs 1 day after TBI. The TBI + vehicle group displayed higher expression of the Nrf2 (P<0.001) and HO-1 (P<0.01) mRNAs than the sham group. ATX substantially increased the expression of the Nrf2 (P<0.05) and HO-1 (P<0.01) mRNAs compared with the TBI + vehicle group; n = 6 animals per group. **P<0.01 and ***P<0.001 compared with the sham group; $^{\#}P$<0.05 and $^{\#\#}P$<0.01 compared with the TBI + vehicle group.

Expression of the Nrf2 mRNA and its downstream factor HO-1

As shown in **Figure 3**, the Nrf2 (P<0.05) and HO-1 (P<0.01) mRNAs were expressed at higher levels in the TBI + ATX group than in the TBI + vehicle group. Higher expression of the Nrf2 (P<0.001) and HO-1 (P<0.01) mRNAs was observed in the TBI + vehicle group than in the sham group.

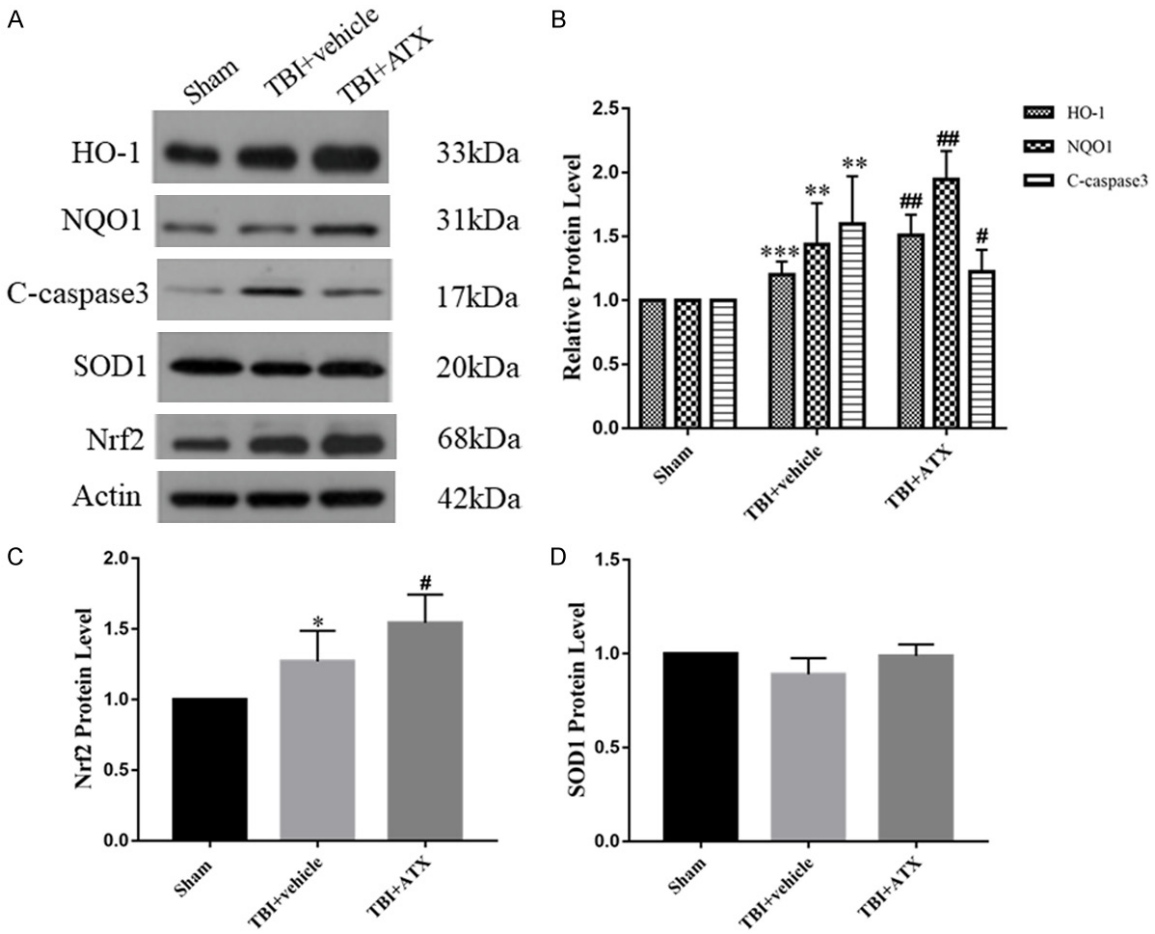

Figure 4. ATX activates the Nrf2/HO-1 pathway and inhibits neuronal apoptosis after TBI. Western blots showing the levels of HO-1, NQO1, C-caspase3, SOD1, and Nrf2 (A) in different groups. Compared with the sham group, levels of the HO-1 (P<0.001), NQO1 (P<0.01), C-caspase3 (P<0.01) (B) and Nrf2 (P<0.05) (C) proteins were increased after TBI, but SOD1 levels were decreased (D). Compared with the TBI + vehicle group, levels of the HO-1 (P<0.01), NQO1 (P<0.01) (B), Nrf2 (P<0.05) (C) and SOD1 (D) proteins were increased in the ATX treatment group, while C-caspase3 levels (P<0.05) (B) were decreased; n = 6 animals per group. *P<0.05, **P<0.01, and ***P<0.001 compared with the sham group; #P<0.05 and ##P<0.01 compared with the TBI + vehicle group.

The inhibitory effect of ATX on oxidative stress in the TBI model and on increasing the levels of the Nrf2 protein and its downstream factors

The level of the SOD1 protein was detected using Western Blot to evaluate the antioxidant capacity of ATX in the mice with TBI. As shown in **Figure 4A** and **4D**, a lower level of the SOD1 protein was detected in the TBI + vehicle group than in the sham group (**Figure 4D**), but the level was higher in the TBI + ATX group, although the difference was not significant. Levels of the HO-1 (P<0.001, **Figure 4B**) and NQO1 (P<0.01, **Figure 4B**) proteins were increased in the TBI + vehicle group compared to the sham group. Furthermore, the HO-1 and NQO1 (both P<0.01, **Figure 4B**) proteins were expressed at higher levels in the ATX treatment group than in the TBI + vehicle group. Compared with the sham group, the Nrf2 protein was expressed at higher levels in the TBI + vehicle group (P<0.05, **Figure 4C**). In addition, higher Nrf2 levels were observed in the ATX treatment group than in the TBI + vehicle group (**Figure 4C**, P<0.05).

ATX exerts an antiapoptotic effect after TBI

Very few TUNEL-positive cells were observed in the sham group. The apoptosis rate in the TBI + vehicle group was significantly higher (P< 0.001, **Figure 5A** and **5B**) than the sham group. However, the rate of apoptosis in the ATX treatment group was significantly lower than in the TBI + vehicle group (P<0.001, **Figure 5A** and

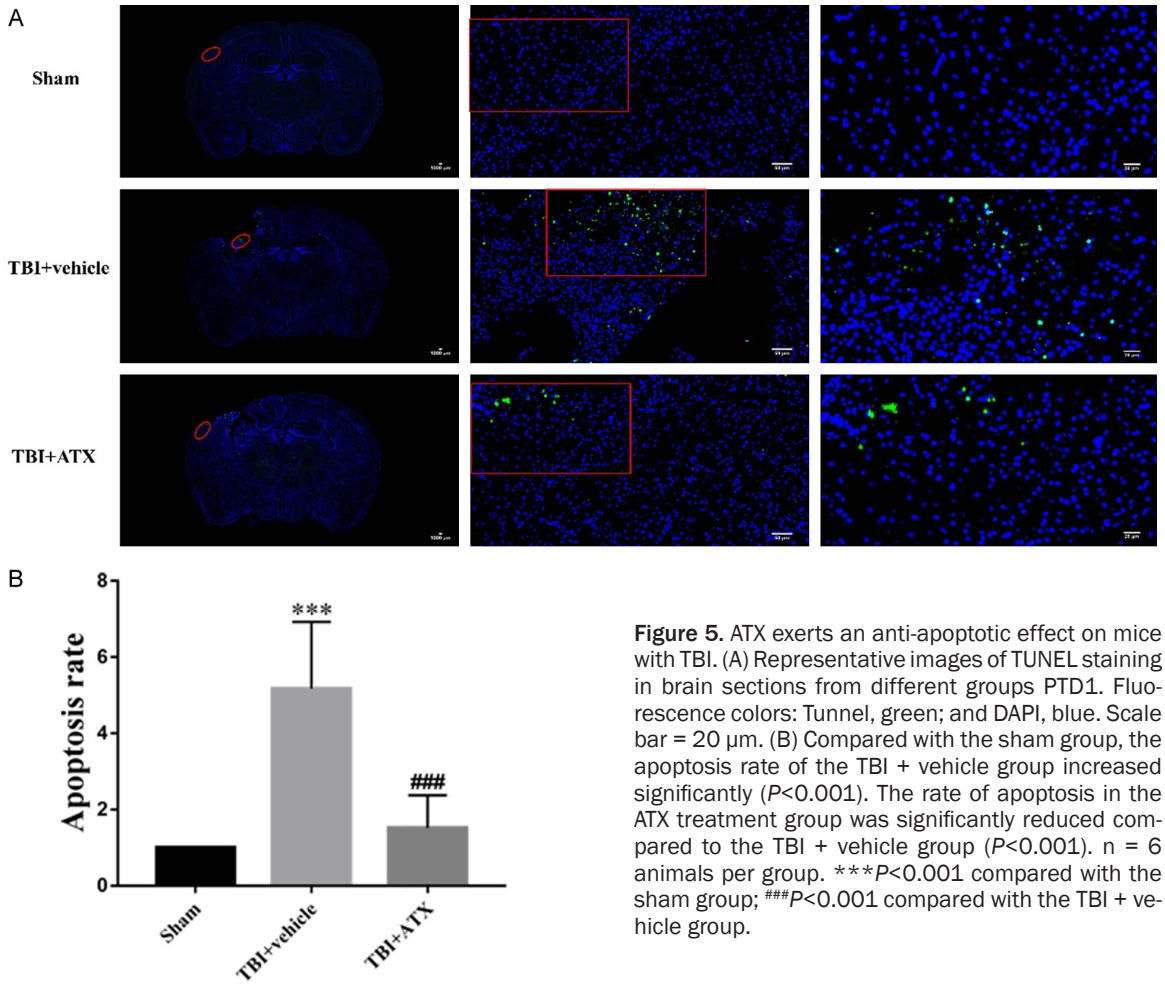

Figure 5. ATX exerts an anti-apoptotic effect on mice with TBI. (A) Representative images of TUNEL staining in brain sections from different groups PTD1. Fluorescence colors: Tunnel, green; and DAPI, blue. Scale bar = 20 μm. (B) Compared with the sham group, the apoptosis rate of the TBI + vehicle group increased significantly (P<0.001). The rate of apoptosis in the ATX treatment group was significantly reduced compared to the TBI + vehicle group (P<0.001). n = 6 animals per group. ***P<0.001 compared with the sham group; ###P<0.001 compared with the TBI + vehicle group.

5B). Thus, ATX exerted an antiapoptotic effect on a mouse model of TBI. Furthermore, the level of the C-caspase3 protein was increased after TBI (P<0.01, **Figure 4A** and **4B**) and decreased after the ATX treatment (P<0.05, **Figure 4A** and **4B**).

Discussion

In our mouse model of TBI, ATX exerted neuroprotective effects, and we assessed the potential role of the Nrf2/HO-1 pathway in this process. Our results are described below. 1) ATX improved the neural function of mice on PTDs 1, 3, and 7. 2) One day after TBI in mice, the levels of the Nrf2 mRNA and protein were increased and induced changes in the levels of the downstream molecules HO-1 and NQO1; and ATX further promoted these changes. 3) One day after TBI in mice, Nrf2 was imported into the nucleus, and ATX increased its nuclear import. Based on these results, ATX may exert neuroprotective effects on a mouse model of TBI by activating the Nrf2/HO-1 pathway.

The neuroprotective and antioxidant functions of ATX have been described in many reports. As shown in the study by Zhang et al., ATX improves the neural function of a mouse model of CCI and alleviates brain edema by regulating the expression of NKCC1 and AQP4 [32]. ATX has also been shown to reduce neuroinflammation leading to neuropathic pain and dyskinesia in rat models of spinal cord injury [37]. ATX activates the Nrf2-ARE pathway to prevent oxidative stress and inflammatory responses and alleviate early brain damage in a rat model of subarachnoid hemorrhage [31]. Based on these studies, ATX exerts neuroprotective effects by attenuating secondary damage after TBI. Similar behavioral changes were also observed in our study. ATX reduced the NSSs of TBI model mice and increased the latency of mice to fall on the rotating rod, indicating that it improved

the neuromotor function of mice. Additionally, in the FST, ATX increased the ability of the mice to struggle during desperation, indicating that it improved the ability of the mice to resist depression after TBI.

Many previous studies have revealed that oxidative stress and the inflammatory response are crucial processes in secondary injury after TBI and are related to most of the pathological changes in the brain and to neurological dysfunction. Based on accumulating evidence, the Nrf2-ARE pathway has neuroprotective anti-inflammatory and antioxidant roles in vivo by upregulating HO-1 and NQO1 after TBI [38, 39]. We assessed the activation of and histological alterations in the Nrf2/HO-1 pathway to determine whether this pathway is involved in the neuroprotective effect of ATX on a mouse model of TBI. We observed higher levels of the Nrf2 and HO-1 mRNAs and proteins after TBI than after the sham surgery; TBI increased Nrf2 nuclear import, as determined by immunofluorescence staining; and ATX promoted this increase in Nrf2 nuclear import and increased the activation of the Nrf2-HO-1 pathway. Furthermore, ATX exerted an inhibitory effect on apoptosis one day after TBI. This finding is consistent with the effects of ATX on a rat model of subarachnoid hemorrhage. However, the specific underlying molecular mechanism of ATX remains unknown.

In addition, since ATX increases the activation of Nrf2 and alleviates oxidative stress and brain damage in a TBI model, the Nrf2/HO-1 pathway may play a key role in ATX-induced neuroprotection [40]. However, the mechanism by which ATX activates the Nrf2/HO-1 signaling pathway is unclear. Nrf2 is a redox-sensitive transcription factor that triggers the expression of phase II antioxidant enzymes under oxidative or electrophilic stimulation to regulate oxidative stress and inflammation [41]. Phase II antioxidant enzymes include HO-1 and NQO1, which are known to protect tissues from injury caused by high oxygen levels [42]. HO-1 and NQO1 are effective antioxidants and detoxifying enzymes that may help relieve oxidative damage and brain damage. ATX increases HO-1 expression through the ERK1/2 pathway, thereby exerting an antioxidant effect on SH-SY5Y cells [43]. ATX ameliorates cardiomyocyte apoptosis after coronary heart disease through the Nrf2/HO-1 pathway [44]. Another study revealed that ATX generates minute amounts of reactive oxygen species (ROS) that subsequently activate Nrf2/HO-1 signaling in human umbilical vein endothelial cells [45]. Based on the data described above, we conclude that the neuroprotective effect of ATX on TBI is likely associated with the activation of the Nrf2/HO-1 pathway.

Conclusions

As shown in the present study, ATX exerts neuroprotective effects on a mouse model of TBI, and we discussed the related mechanisms. ATX reduces secondary damage after TBI, improving the neuromotor function of mice after TBI and reducing TBI-induced apoptosis, effects that are likely related to the activation of the Nrf2/HO-1 pathway. Further extensive preclinical research on the basic mechanism by which ATX treats TBI is needed. According to our study, ATX is likely to be a prospective drug for the treatment of secondary injury after TBI.

Disclosure of conflict of interest

None.

Address correspondence to: Baiyun Liu, Beijing Tiantan Hospital, Capital Medical University, Beijing 100070, China; Beijing Key Laboratory of Central Nervous System Injury, Beijing Neurosurgical Institute, Capital Medical University, Beijing 100070, China; Nerve injury and Repair Center of The Beijing Institute for Brain Disorders, Beijing 100070, China; China National Clinical Research Center for Neurological Diseases, Beijing 100070, China. Tel: +86-13801375372; E-mail: liubaiyun1212@163.com

References

[1] Maas A, Menon DK, Adelson PD, Andelic N, Bell MJ, Belli A, Bragge P, Brazinova A, Buki A, Chesnut RM, Citerio G, Coburn M, Cooper DJ, Crowder AT, Czeiter E, Czosnyka M, Diaz-Arrastia R, Dreier JP, Duhaime AC, Ercole A, van Essen TA, Feigin VL, Gao G, Giacino J, Gonzalez-Lara LE, Gruen RL, Gupta D, Hartings JA, Hill S, Jiang JY, Ketharanathan N, Kompanje E, Lanyon L, Laureys S, Lecky F, Levin H, Lingsma HF, Maegele M, Majdan M, Manley G, Marsteller J, Mascia L, McFadyen C, Mondello S, Newcombe V, Palotie A, Parizel PM, Peul W, Piercy J, Polinder S, Puybasset L, Rasmussen TE, Rossaint R, Smielewski P, Soderberg J, Stanworth SJ, Stein MB, von Steinbuchel N, Stewart W, Steyerberg EW, Stocchetti N, Synnot A, Te AB, Tenovuo O, Theadom A, Tibboel D, Videtta W,

Wang K, Williams WH, Wilson L and Yaffe K. Traumatic brain injury: integrated approaches to improve prevention, clinical care, and research. Lancet Neurol 2017; 16: 987-1048.
[2] Mao X, Xie S and Liu B. Neurotrauma in China. World Neurosurg 2016; 92: 552-558.
[3] Liu Z, Wang H, Shi X, Li L, Zhou M, Ding H, Yang Y, Li X and Ding K. DL-3-n-Butylphthalide (NBP) provides neuroprotection in the mice models after traumatic brain injury via Nrf2-ARE signaling pathway. Neurochem Res 2017; 42: 1375-1386.
[4] Mayeux JP, Teng SX, Katz PS, Gilpin NW and Molina PE. Traumatic brain injury induces neuroinflammation and neuronal degeneration that is associated with escalated alcohol self-administration in rats. Behav Brain Res 2015; 279: 22-30.
[5] Mao X, Terpolilli NA, Wehn A, Cheng S, Hellal F, Liu B, Seker B and Plesnila N. Progressive histopathological damage occurring up to one year after experimental traumatic brain injury is associated with cognitive decline and depression-like behavior. J Neurotrauma 2020; 37: 1331-1341.
[6] Bramlett HM and Dietrich WD. Long-term consequences of traumatic brain injury: current status of potential mechanisms of injury and neurological outcomes. J Neurotrauma 2015; 32: 1834-1848.
[7] Khatri N, Thakur M, Pareek V, Kumar S, Sharma S and Datusalia AK. Oxidative stress: major threat in traumatic brain injury. CNS Neurol Disord Drug Targets 2018; 17: 689-695.
[8] Zheng B, Zhang S, Ying Y, Guo X, Li H, Xu L and Ruan X. Administration of Dexmedetomidine inhibited NLRP3 inflammasome and microglial cell activities in hippocampus of traumatic brain injury rats. Biosci Rep 2018; 38: 1-11.
[9] Li Z, Zeng G, Zheng X, Wang W, Ling Y, Tang H and Zhang J. Neuroprotective effect of formononetin against TBI in rats via suppressing inflammatory reaction in cortical neurons. Biomed Pharmacother 2018; 106: 349-354.
[10] Zhang M, Huang LL, Teng CH, Wu FF, Ge LY, Shi YJ, He ZL, Liu L, Jiang CJ, Hou RN, Xiao J, Zhang HY and Chen DQ. Isoliquiritigenin provides protection and attenuates oxidative stress-induced injuries via the Nrf2-ARE signaling pathway after traumatic brain injury. Neurochem Res 2018; 43: 2435-2445.
[11] Kumar A, Stoica BA, Loane DJ, Yang M, Abulwerdi G, Khan N, Kumar A, Thom SR and Faden AI. Microglial-derived microparticles mediate neuroinflammation after traumatic brain injury. J Neuroinflammation 2017; 14: 47.
[12] Frati A, Cerretani D, Fiaschi AI, Frati P, Gatto V, La Russa R, Pesce A, Pinchi E, Santurro A, Fraschetti F and Fineschi V. Diffuse axonal injury and oxidative stress: a comprehensive review. Int J Mol Sci 2017; 18: 1-20.
[13] Ernst IM, Wagner AE, Schuemann C, Storm N, Hoppner W, Doring F, Stocker A and Rimbach G. Allyl-, butyl- and phenylethyl-isothiocyanate activate Nrf2 in cultured fibroblasts. Pharmacol Res 2011; 63: 233-240.
[14] Cullinan SB, Gordan JD, Jin J, Harper JW and Diehl JA. The Keap1-BTB protein is an adaptor that bridges Nrf2 to a Cul3-based E3 ligase: oxidative stress sensing by a Cul3-Keap1 ligase. Mol Cell Biol 2004; 24: 8477-8486.
[15] Zhang DD, Lo SC, Cross JV, Templeton DJ and Hannink M. Keap1 is a redox-regulated substrate adaptor protein for a Cul3-dependent ubiquitin ligase complex. Mol Cell Biol 2004; 24: 10941-10953.
[16] Zhang M, An C, Gao Y, Leak RK, Chen J and Zhang F. Emerging roles of Nrf2 and phase II antioxidant enzymes in neuroprotection. Prog Neurobiol 2013; 100: 30-47.
[17] Hur W and Gray NS. Small molecule modulators of antioxidant response pathway. Curr Opin Chem Biol 2011; 15: 162-173.
[18] Jin W, Wang H, Ji Y, Hu Q, Yan W, Chen G and Yin H. Increased intestinal inflammatory response and gut barrier dysfunction in Nrf2-deficient mice after traumatic brain injury. Cytokine 2008; 44: 135-140.
[19] Li F, Wang X, Zhang Z, Zhang X and Gao P. Dexmedetomidine attenuates neuroinflammatory-induced apoptosis after traumatic brain injury via Nrf2 signaling pathway. Ann Clin Transl Neurol 2019; 6: 1825-1835.
[20] Caglayan B, Kilic E, Dalay A, Altunay S, Tuzcu M, Erten F, Orhan C, Gunal MY, Yulug B, Juturu V and Sahin K. Allyl isothiocyanate attenuates oxidative stress and inflammation by modulating Nrf2/HO-1 and NF-kappaB pathways in traumatic brain injury in mice. Mol Biol Rep 2019; 46: 241-250.
[21] Chen G, Fang Q, Zhang J, Zhou D and Wang Z. Role of the Nrf2-ARE pathway in early brain injury after experimental subarachnoid hemorrhage. J Neurosci Res 2011; 89: 515-523.
[22] Lu XY, Wang HD, Xu JG, Ding K and Li T. Deletion of Nrf2 exacerbates oxidative stress after traumatic brain injury in mice. Cell Mol Neurobiol 2015; 35: 713-721.
[23] Lorenz RT and Cysewski GR. Commercial potential for Haematococcus microalgae as a natural source of astaxanthin. Trends Biotechnol 2000; 18: 160-167.
[24] Kupcinskas L, Lafolie P, Lignell A, Kiudelis G, Jonaitis L, Adamonis K, Andersen LP and Wadstrom T. Efficacy of the natural antioxidant astaxanthin in the treatment of functional dyspepsia in patients with or without Helicobacter pylori infection: a prospective, randomized,

double blind, and placebo-controlled study. Phytomedicine 2008; 15: 391-399.
[25] Hussein G, Sankawa U, Goto H, Matsumoto K and Watanabe H. Astaxanthin, a carotenoid with potential in human health and nutrition. J Nat Prod 2006; 69: 443-449.
[26] Palozza P, Torelli C, Boninsegna A, Simone R, Catalano A, Mele MC and Picci N. Growth-inhibitory effects of the astaxanthin-rich alga Haematococcus pluvialis in human colon cancer cells. Cancer Lett 2009; 283: 108-117.
[27] Higuera-Ciapara I, Felix-Valenzuela L and Goycoolea FM. Astaxanthin: a review of its chemistry and applications. Crit Rev Food Sci Nutr 2006; 46: 185-196.
[28] Yuan JP, Peng J, Yin K and Wang JH. Potential health-promoting effects of astaxanthin: a high-value carotenoid mostly from microalgae. Mol Nutr Food Res 2011; 55: 150-165.
[29] Fassett RG and Coombes JS. Astaxanthin, oxidative stress, inflammation and cardiovascular disease. Future Cardiol 2009; 5: 333-342.
[30] Chan KC, Mong MC and Yin MC. Antioxidative and anti-inflammatory neuroprotective effects of astaxanthin and canthaxanthin in nerve growth factor differentiated PC12 cells. J Food Sci 2009; 74: H225-231.
[31] Wu Q, Zhang XS, Wang HD, Zhang X, Yu Q, Li W, Zhou ML and Wang XL. Astaxanthin activates nuclear factor erythroid-related factor 2 and the antioxidant responsive element (Nrf2-ARE) pathway in the brain after subarachnoid hemorrhage in rats and attenuates early brain injury. Mar Drugs 2014; 12: 6125-6141.
[32] Zhang M, Cui Z, Cui H, Cao Y, Zhong C and Wang Y. Astaxanthin alleviates cerebral edema by modulating NKCC1 and AQP4 expression after traumatic brain injury in mice. BMC Neurosci 2016; 17: 60.
[33] Ji X, Peng D, Zhang Y, Zhang J, Wang Y, Gao Y, Lu N and Tang P. Astaxanthin improves cognitive performance in mice following mild traumatic brain injury. Brain Res 2017; 1659: 88-95.
[34] Mao X, Hao S, Zhu Z, Zhang H, Wu W, Xu F and Liu B. Procyanidins protects against oxidative damage and cognitive deficits after traumatic brain injury. Brain Inj 2015; 29: 86-92.
[35] Mao X, Miao G, Tao X, Hao S, Zhang H, Li H, Hou Z, Tian R, Lu T, Ma J, Zhang X, Cheng H and Liu B. Saikosaponin a protects TBI rats after controlled cortical impact and the underlying mechanism. Am J Transl Res 2016; 8: 133-141.
[36] Jiang L, Xia QJ, Dong XJ, Hu Y, Chen ZW, Chen K, Wang KH, Liu J and Wang TH. Neuroprotective effect of breviscapine on traumatic brain injury in rats associated with the inhibition of GSK3beta signaling pathway. Brain Res 2017; 1660: 1-9.
[37] Fakhri S, Dargahi L, Abbaszadeh F and Jorjani M. Astaxanthin attenuates neuroinflammation contributed to the neuropathic pain and motor dysfunction following compression spinal cord injury. Brain Research Bulletin 2018; 143: 217-224.
[38] Miller DM, Singh IN, Wang JA and Hall ED. Nrf2-ARE activator carnosic acid decreases mitochondrial dysfunction, oxidative damage and neuronal cytoskeletal degradation following traumatic brain injury in mice. Exp Neurol 2015; 264: 103-110.
[39] Chandran R, Kim T, Mehta SL, Udho E, Chanana V, Cengiz P, Kim H, Kim C and Vemuganti R. A combination antioxidant therapy to inhibit NOX2 and activate Nrf2 decreases secondary brain damage and improves functional recovery after traumatic brain injury. J Cereb Blood Flow Metab 2018; 38: 1818-1827.
[40] Dai W, Wang H, Fang J, Zhu Y, Zhou J, Wang X, Zhou Y and Zhou M. Curcumin provides neuroprotection in model of traumatic brain injury via the Nrf2-ARE signaling pathway. Brain Res Bull 2018; 140: 65-71.
[41] Ahmed SM, Luo L, Namani A, Wang XJ and Tang X. Nrf2 signaling pathway: pivotal roles in inflammation. Biochim Biophys Acta Mol Basis Dis 2017; 1863: 585-597.
[42] Funakohi-Tago M, Sakata T, Fujiwara S, Sakakura A, Sugai T, Tago K and Tamura H. Hydroxytyrosol butyrate inhibits 6-OHDA-induced apoptosis through activation of the Nrf2/HO-1 axis in SH-SY5Y cells. Eur J Pharmacol 2018; 834: 246-256.
[43] Wang HQ, Sun XB, Xu YX, Zhao H, Zhu QY and Zhu CQ. Astaxanthin upregulates heme oxygenase-1 expression through ERK1/2 pathway and its protective effect against beta-amyloid-induced cytotoxicity in SH-SY5Y cells. Brain Res 2010; 1360: 159-167.
[44] Xue Y, Sun C, Hao Q and Cheng J. Astaxanthin ameliorates cardiomyocyte apoptosis after coronary microembolization by inhibiting oxidative stress via Nrf2/HO-1 pathway in rats. Naunyn Schmiedebergs Arch Pharmacol 2019; 392: 341-348.
[45] Niu T, Xuan R, Jiang L, Wu W, Zhen Z, Song Y, Hong L, Zheng K, Zhang J, Xu Q, Tan Y, Yan X and Chen H. Astaxanthin induces the Nrf2/HO-1 antioxidant pathway in human umbilical vein endothelial cells by generating trace amounts of ROS. J Agric Food Chem 2018; 66: 1551-1559.